Parametric Numerical Analysis of Fire-Induced Pressure Variations in a Well-Confined and Mechanically Ventilated Compartment

T. Beji*, J. Degroote, B. Merci

Department of Flow, Heat and Combustion Mechanics, Ghent University-UGent, Sint-Pietersnieuwstraat 41, 9000 Ghent, Belgium

Abstract

The investigation of a fire in a well-confined and mechanically ventilated compartment is of primary importance for the nuclear industry. In normal operating conditions, a ventilation network system is set-up to ensure confinement via an appropriate pressure cascade. In the event of a fire, the subsequent pressure build-up alters the confinement level significantly and therefore changes the level of safety of the installation. The fire-induced pressure variations depend mainly on the: (1) HRR (Heat Release Rate) history of the fire, (2) heat losses to the walls, (3) leakage area, and (4) operating conditions of the fans. A numerical parametric analysis on the latter three parameters, using the Fire Dynamics Simulator (FDS 5.5.3), have shown that a change in the initial ventilation parameters (*i.e.* operating conditions of the fans and/or leaks), which can be sometimes difficult to determine, may lead to substantial changes in the pressure profiles. However, only a change in the thermal boundary conditions (*i.e.* presence or no of insulation) produces significant changes in the gas temperature.

Introduction

An intensive effort is undertaken by several parties in order to enhance the level of fire safety in Nuclear Power Plants. The understanding of fire development in nuclear facilities is continuously improved by research programs and projects such as PRISME [1], which is an international project involving several OECD member countries. The large experimental program relies on large-scale facilities and addresses several aspects such as: (i) the characterization of fire sources (*e.g.* pool fires [2] or electrical cabinets [3]), (ii) the effects of confinement and mechanical ventilation on the mass loss rate [4-6] and the pressure profiles [7], and (iii) the multi-compartment configurations [8]. The analysis of the experimental data is complemented by numerical simulations performed using several codes in order to evaluate them and identify possible weaknesses and points for improvement in design and hazard analysis [9].

Nuclear facilities are usually equipped with a ventilation network system that ensures dynamic confinement in order to contain the potential release of radioactive materials and avoid dispersion to the outside. In the event of a fire, the subsequent pressure build-up within the fire room alters significantly the confinement level and therefore poses significant hazards, including the damage of mechanical safety devices [7]. The interaction of fire dynamics with the mechanical ventilation system in a well-confined room has been experimentally investigated in [7]. It was found that overpressure peaks of up to 3000 Pa can be reached within few seconds. Furthermore, it might take several minutes before normal ventilation conditions are reached again. The fire-induced pressure variations depend mainly on: (1) the HRR (Heat Release Rate) history of the fire, (2) heat losses to the walls, (3) leakage area, and (4) operating conditions of the fans. The increasing CFD (Computational Fluid Dynamics) capabilities allow widening the range of experimentally examined fire scenarios. However, continuous extensive validation studies need to be conducted. In [10], numerical simulations were performed for the case of a well confined and mechanically ventilated compartment using the Fire Dynamics Simulator (FDS 5.5.3) [11]. A good agreement between the experimental data [10] and the numerical results was obtained. Nevertheless, the authors pointed out the necessity of further investigations.

Specific Objectives

In the numerical work (using FDS 5.5.3) presented here, a sensitivity study is performed in order to highlight the effect of three parameters on the fire-induced pressure variations in a well-confined and mechanically-ventilated compartment. These parameters are: (1) heat losses to walls, (2) leakage area, and (3) operating conditions of the fans (inlet and exhaust branches).

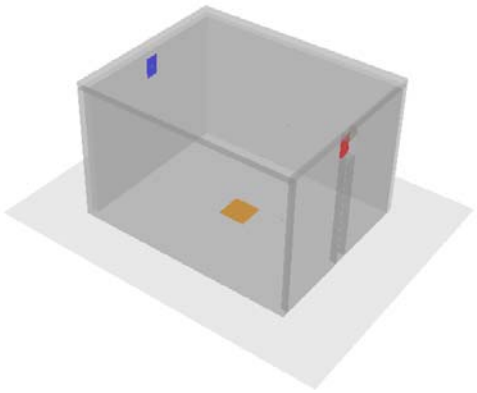

Figure 1. Geometrical configuration.

* Corresponding author: Tarek.Beji@UGent.be

The geometrical configuration considered in this paper is similar to [7]. It consists of a tightly-sealed compartment (dimensions: 6 m × 5 m × 4 m high) made of 20-cm thick concrete walls and connected to the open atmosphere via one inlet and one outlet branches (see Fig. 1). Each branch is equipped with a fan. Both ventilation ducts (dimensions: 0.4 m × 0.6 m) are placed in the centre of two opposite walls at 3.20 m height above floor levels. Air leakage from the walls is set-up. The total computational domain is 10 m × 8 m × 6 m high.

A propane fire (default fuel in FDS) with a 0.8 × 0.8 m^2 square burner, placed in the centre of the room, was prescribed according to the HRR curve shown in Fig. 2. An initial period of 1 minute before ignition was set to have a stabilized flow and an initial background pressure, p_0, inside the room based on the operating conditions of the fans and the leakage area.

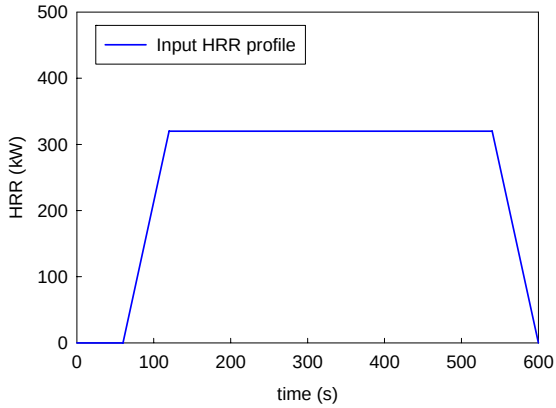

Figure 2. FDS input HRR profile.

After ignition, the fire increases linearly to reach 320 kW in 1 minute and then remains steady during 8 minutes. Finally the HRR decreases to 0 kW in one minute.

Two thermal boundary conditions have been used. Most of the calculations were performed with 20-cm thick concrete walls as mentioned earlier. The effect of the thermal boundary condition was investigated by adding, in one simulation, a 5-cm rock wool insulating layer at the inner side of the walls. Material properties (*i.e.* thickness, δ, conductivity, k, specific heat, c_p, and density, ρ) are provided in Table 1.

Table 1. Thermal boundary properties.

Material	δ (m)	k (W/m.K)	c_p (kJ/kg.K)	ρ (kg/m^3)
Concrete	0.20	1.500	0.736	2430
Rock wool	0.05	0.102	0.840	140

In the event of a fire in well-confined and mechanically ventilated compartments, pressure-related effects have a substantial influence on the level of ventilation induced by the fans, which extract vitiated air and inject fresh air. The basic FDS equation set assumes pressure to be composed of a "background" component $\bar{p}(z,t)$, plus a perturbation, $\tilde{p}(x,t)$ [11]. The former is the hydrostatic pressure. The latter is the flow-induced pressure calculated by FDS at each time step. In order to simulate a flow between two volumes at different pressures, each volume must be defined as a "pressure zone" having its own background pressure, which increases and decreases due to the effects of fans, leaks and/or fire. In the configuration considered in this work (see Fig. 1), one zone was assigned to the compartment (index 1). The surrounding environment at ambient pressure is considered as a separate pressure zone by default (index 0).

The volume flow, $\dot{V}$, supplied by a fan is given by:

$$\dot{V} = \dot{V}_{max}\, sign\left(\Delta p_{max} - \Delta p\right)\sqrt{\frac{\left|\Delta p - \Delta p_{max}\right|}{\Delta p_{max}}} \qquad (1)$$

where $\dot{V}_{max}$ is the maximum volume flow rate (at $\Delta p = 0$ Pa), Δp_{max} the maximum pressure difference that the fan can operate on, and Δp the pressure difference between adjacent compartments. The maximum volume flow rates were set up at 0.096 m^3/s, for the inlet and 0.144 m^3/s for the outlet.

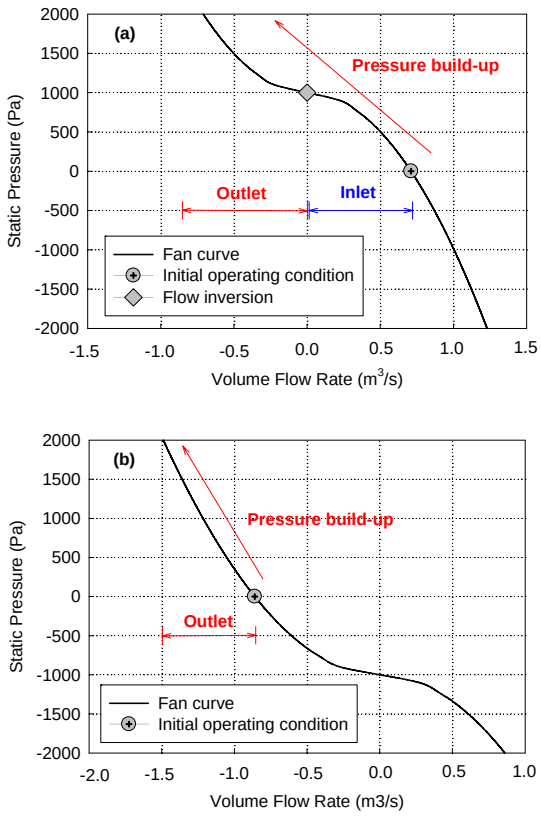

Figure 3. Fan curves at an (a) inlet and (b) outlet ducts.

The default value for Δp_{max} was 1000 Pa. Two additional values were used (500 Pa and 1500 Pa) to study the effect of this parameter.

Figure 3 shows an example of fan curves using the model provided in Eq. (1). It can be seen in Fig. 3a that for an inlet duct (positive flow rate), a pressure build-up induced by a fire will cause a decrease in the volume flow rate until it becomes zero at Δp_{max} and then negative (*i.e.* backflow) afterwards. For the extraction duct (see Fig. 3b), the pressure build-up will enhance the extraction rate (*i.e.* increased volume flow rate in absolute value). It is the overall flow behaviour at the two ducts in conjunction with the HRR of the fire that will determine the induced pressure profile. In the work presented here, only the inlet and outlet fans are modeled. However, in the pre-release version of FDS 6 [12], it is possible to set-up the full ventilation network (with the associated nodes, pressures and volume flow rates further downstream). This option is not considered in this work.

Leaks might have a significant effect on the fire-induced pressure profiles. The volume flow through a leak of area A_L is given by:

$$\dot{V}_{leak} = A_L \, sign(\Delta p) \sqrt{2 \frac{|\Delta p|}{\rho_0}} \qquad (2)$$

where ρ_0 is the ambient density ($\rho_0 = 1.2 \; kg/m^3$).

In [10], the leakage area was estimated to be $A_L = 4$ cm^2. Such value suggests that the facility used in the PRISME program is very tightly sealed. In order to perform a sensitivity study, the additional bounding values of 0 and 10 cm^2 were tested. It is interesting to note that in [13] the estimated leakage area from the exterior building walls for a tight building represents 0.05 % of the wall area. This represents $A_L = 44$ cm^2 for the compartment considered in this study, which is 11 times the value used in [10]. Therefore, this value is also included in the sensitivity study of A_L.

Table 2 provides the list of simulations performed in this work. The base case is highlighted in grey shading. The other simulations were undertaken to examine the effects of:

- mesh size,
- insulation,
- maximum operating pressure of the fans, and
- leakage area.

Table 2. List of the simulations.

SIM	***Mesh***	***Walls***	Δp_{max} **(Pa)**	A_L **(cm^2)**
SIM_0_10	10 cm	concrete	1000	4
SIM_0_20	20 cm	concrete	1000	4
SIM_W	20 cm	insulated	1000	4
SIM_F_1	20 cm	concrete	500	4
SIM_F_2	20 cm	concrete	1500	4
SIM_L_1	20 cm	concrete	1000	0
SIM_L_2	20 cm	concrete	1000	10
SIM_L_3	20 cm	concrete	1000	44

Results and Discussion

First, a description of the base case scenario (SIM_0_20, see Table 2) is performed. Before ignition, the volume flow rate of the outlet, resp. inlet, fan is stabilized at 430 m^3/h, resp. 396 m^3/h (see Fig. 4). The difference corresponds to the volume flow rate at the leak. These operating conditions correspond to a renewal rate of Tr = 3.58 h^{-1}. The renewal rate is defined as the volumetric flow rate divided by the volume of the enclosure (120 m^3 in this case). The initial background pressure inside the room is stabilized at p_0 = -315 Pa. When the fire started, the room pressure rose progressively until it reached, 64 s later, an overpressure peak, $\Delta p = p - p_0$, of 2224 Pa (see Fig. 5). In the mean time, 30 s after ignition, due to pressure build-up in the room caused by the fire, a flow inversion is observed at the inlet branch (see Fig. 4): smoke is flowing backward out of the fan duct. As both fans are now extracting smoke out of the room, the pressure decreases and reaches a quasi steady-state between t = 360 s and t = 540 s with an average value of 0 Pa. When the fire HRR starts to decrease (at t = 540 s), pressure decreases until it reaches a low pressure peak of – 1259 Pa at the end of the simulation, which corresponds to complete extinction of the fire.

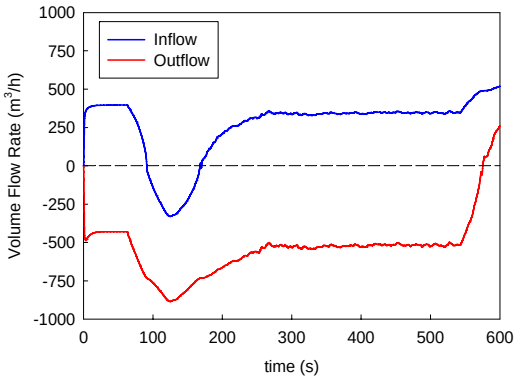

Figure 4. Volume flow rates at the inlet and outlet ducts for the base case simulation (SIM_0_20).

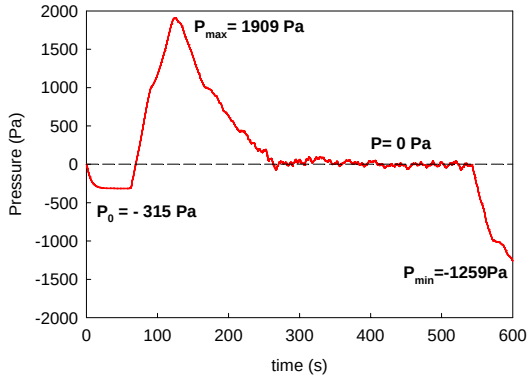

Figure 5. Pressure Profile inside the room for the base case simulation (SIM_0_20).

It is important to note that the fire considered here is overventilated. The amount of oxygen supplied into the

room through mechanical ventilation is sufficient to sustain the burning prescribed as input. Figure 6 confirms that the same HRR profile is recovered at the end of the simulation. Furthermore, oxygen concentration levels displayed in Fig. 7 are above the extinction limit (*i.e.* 10%) incorporated in the FDS algorithm. Additional simulations (which are not shown here) confirm that FDS is able to "detect" underventilated conditions in case of low oxygen volume fractions that do not sustain burning.

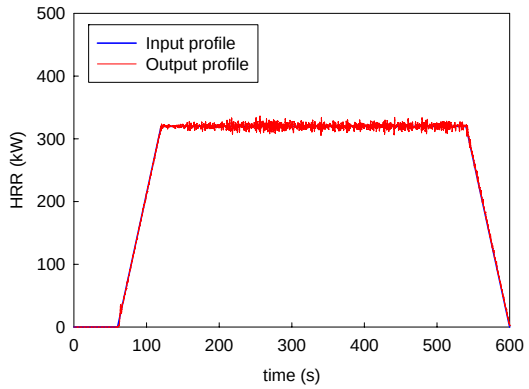

Figure 6. Input and output HRR profiles for the base case simulation (SIM_0_20).

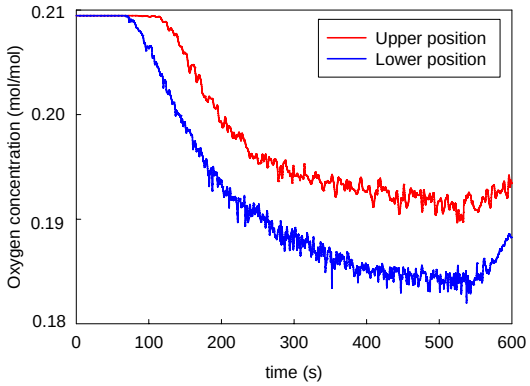

Figure 7. Oxygen concentration profiles for the base case simulation (SIM_0_20).

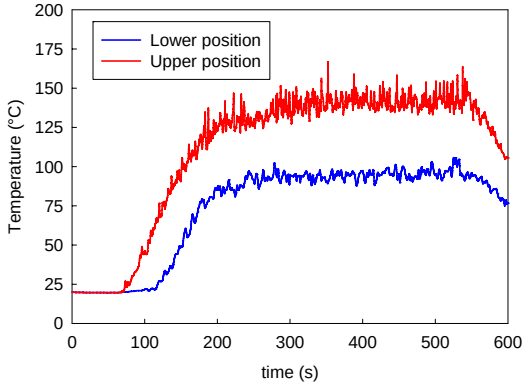

Figure 8. Temperature profiles for the base case simulation (SIM_0_20).

Similarly to the HRR, volume flow rates and pressure, the temperature reaches a steady-state stage with a value of 142 °C at an upper position and 96 °C at a lower position (see Fig. 8).

All the results of the simulations carried out after the base case simulation (SIM_0_20) exhibit qualitatively the same profiles shown in Figs. 4 to 8. However, there are significant differences, mainly in the pressure values. Table 3 displays the pressure results for each simulation in terms of overpressure peak, steady state pressure and low pressure along with their relative deviation, ε, from the results of SIM_0_20. Table 4 displays similarly the results for the steady-state temperature.

A comparison of the results of the base case scenario with the results of the 'fine mesh' simulation (*i.e.* SIM_0_10) shows relative deviations of less than 9 % in the pressure and temperature results. The simulation time (total CPU) increased from 1.35 hr to 26.81 hr. On the basis of these results, a mesh of 20 cm was considered to give a good compromise between accuracy and required computational time.

Table 3. Pressure results.

	Overpressure		Steady-state		Low pressure	
	Δp (Pa)	ε (%)	Δp (Pa)	ε (%)	Δp (Pa)	ε (%)
SIM_0_20	2224		315		-944	
SIM_0_10	2031	-8.7	322	-0.9	-941	-0.3
SIM_W	2641	18.8	444	36.6	-945	0.1
SIM_F_1	2528	13.7	367	12.9	-964	2.1
SIM_F_2	1909	-14.2	239	-26.5	-922	-2.3
SIM_L_1	3109	39.8	455	40.0	-1337	41.6
SIM_L_2	1239	-44.3	176	-45.8	-506	-46.4
SIM_L_3	1057	-52.5	55	-83.1	-805	-14.7

Table 4. Steady-state temperature results.

	Upper temperature		Lower temperature	
	T_u (°C)	ε (%)	T_l (°C)	ε (%)
SIM_0_20	142		96	
SIM_0_10	140	-1.4	90	-6.3
SIM_W	192	35.2	138	43.8
SIM_F_1	145	2.1	95	-1.0
SIM_F_2	141	-0.7	95	-1.0
SIM_L_3	142	0.0	96	0.0
SIM_L_2	143	0.7	95	-1.0
SIM_L_1	144	1.4	96	0.0

The pressure equation formulated in [7] reads:

$$\frac{V}{\gamma - 1}\frac{d}{dt}P = \dot{Q}_f - \dot{Q}_w + \dot{Q}_v \qquad (3)$$

where V is the volume of the compartment, γ the isentropic coefficient of the gas, $\dot{Q}_f$ the fire HRR, $\dot{Q}_w$ the thermal losses through walls and $\dot{Q}_v$ the overall heat transfer due to ventilation (including leakage areas).

Obviously, the insulation of the walls reduces thermal losses to the boundaries, $\dot{Q}_w$, which induces increased pressures. However, as stated earlier, increased pressures enhance smoke extraction and therefore pressure relief through the ducts. The objective here was to investigate to what extent these two opposed effects influence the overpressure peak. It was found that the volume flows at the ducts in SIM_W started to deviate from the base case (*i.e.* no insulation) at flow inversion time with enhanced extraction because of higher pressures for the insulated case. The overpressure peak and the stabilization of the pressure occurred at almost the same time but with substantially increased values by 18.8 % for the overpressure and 36.6 % for the steady-state pressure. As expected, due to the insulation the gas temperature was higher by around 40 % for the insulated case (see Table 4).

The maximum pressure difference that the fan can operate on can have also a non-negligible effect on the overpressure peak and steady state pressure because of the subsequent differences in the volume flow rates and the overall heat transfer due to ventilation, $\dot{Q}_v$. Results displayed in Table 3 show that for a range of 500 to 1500 Pa in $\Delta p_{\max}$ the overpressure peak varies between 1900 and 2550 Pa. There are also significant differences in the steady-state pressure. Therefore it is important to know the characteristics of the fan in design calculations in order to minimize the uncertainties in the calculated compartment pressures.

The range of values considered for the leakage area resulted in substantial differences. The most significant difference was observed for A_L = 44 cm^2 where there was no flow inversion because the pressure within the fire compartment remained around 1000 Pa (the maximum pressure difference that the fan can operate on). This value represents a deviation of more than -50 % in the overpressure peak from the base case (A_L = 4 cm^2). Deviations of around -44 % and 40 % were obtained for leakage areas of 10 cm^2 and 0 cm^2.
It seems that the value of A_L = 44 cm^2 calculated on the basis of the SFPE table [13] is not suitable for nuclear installations, which (similarly to sub-marines for example) are much tighter than regular buildings.

Conclusions

The interaction of fire with the mechanical ventilation network in a well-confined room is a scenario of particular interest for the nuclear industry. It has been numerically investigated via the Fire Dynamics Simulator, FDS (5.5.3). The numerical set-up was first described for a base case. The results have shown that FDS is able to qualitatively reproduce transient profiles of pressures and predict important phenomena such as backflows in inlet pipes.
Additional simulations have shown that:

1. For a known prescribed HRR, a mesh size of 20 cm gives an acceptable compromise between accuracy and computational time;
2. A change in the ventilation parameters (*i.e.* operating conditions of the fans and/or leaks), which can be sometimes difficult to determine, may lead to substantial changes in the pressure profiles. However, only a change in the thermal boundary conditions (*i.e.* presence or no of insulation) produces significant changes in the gas temperature.

The scenario considered here is an overventilated fire. Future calculations will be carried out for underventilated conditions where the prediction of the operating ventilation conditions is more crucial to correctly predict the fire development. Furthermore, the numerical data will be compared to available experimental data in order to quantify the deviations in one and multi-room configurations.

Acknowledgements

This research was funded by Bel V in the framework of a cooperation with the University of Gent (UGent), contract ref. number: A12/TT/0617.

References

[1] L. Rigollet, N. Noterman, E. Gorza, A. Siccama, J. Peco, T. Ito, M. Röwekamp, A. Bounagui, G. Lamarre, L. Gay, L. Audouin, R. Gonzalez, H. Prétrel, S. Suard, Organisation for Economic Co-operation and Development (OECD) Report NEA/CSNI/R(2012)14, 2012.
[2] H. Prétrel, W. Le Saux, L. Audouin, (2013) Fire Safety J.
[3] M. Coutin, W. Plumecoq, S. Melis, L. Audouin, Fire Safety J. 52 (2012) 34-45.
[4] H. Prétrel, P. Querre, M. Forestier, in: Proceedings of the eight International Symposium, International Association for Fire Safety Science, 2005, p.1217-1228.
[5] W. Le Saux, H. Prétrel, C. Lucchesi, P. Guillou, in: Proceedings of the ninth International Symposium, International Association for Fire Safety Science, 2008, p. 943-954.
[6] S. Melis, L. Audouin, in: Proceedings of the ninth International Symposium, International Association for Fire Safety Science, 2008, p. 931-942.
[7] H. Prétrel, W. Le Saux, L. Audouin, Fire Safety J. 52 (2012) 11-24.
[8] H. Prétrel, L. Audouin, in: Proceedings of the tenth International Symposium, International Association for Fire Safety Science, 2011, p. 1015-1027.
[9] L. Audouin, L. Chandra, J.L. Consalvi, L. Gay, E. Gorza, V. Hohm, S. Hostikka, T. Ito, W. Klein-Hessling, C. Lallemand, T. Magnusson, N. Noterman, J.S. Park, J. Peco, L. Rigollet, S. Suard, P. Van-Hees, Nucl. Eng. Des. 241 (2011) 18-31.
[10] J. Wahlqvist, P. Van Hees, in: Posters of the tenth International Symposium, International Association for Fire Safety Science, 2011.
[11] K. McGrattan, B. Klein, S. Hostikka, J. Floyd, Fire Dynamics Simulator (Version 5) User's Guide, Report No. NIST Special Publication 1019-5, 2009.

[12] K. McGrattan, B. Klein, S. Hostikka, J. Floyd, Fire Dynamics Simulator (Version 6) User's Guide, Report No. NIST Special Publication 1019, 2012.
[13] J.H. Klote, Smoke Control, third ed., SFPE Handbook of Fire Protection Engineering, National Fire Protection Association, Quincy, MA, 2002. p. 4-282.